EFFECT OF PARTICLE SIZE, BINDER CONTENT AND HEAT TREATMENT ON MECHANICAL PROPERTIES OF 13-93 BIOACTIVE GLASS SCAFFOLDS

Krishna C. R. Kolan[1], Ming C. Leu[1], Gregory E. Hilmas[2] and Mariano Velez[3]

[1]Department of Mechanical and Aerospace Engineering, Missouri University of Science and Technology, Rolla, MO 65409
[2]Department of Materials Science and Engineering, Missouri University of Science and Technology, Rolla, MO 65409
[3]Mo-Sci Corporation, Rolla, MO 65401

Abstract

Particle size, binder content and the post-processing schedule are important parameters that affect the microstructure, and, hence, the mechanical properties of parts produced using the indirect selective laser sintering process. 13-93 bioactive glass, with mean particle sizes ranging from 10 µm to 44 µm, is mixed with different amounts of stearic acid binder to fabricate green scaffolds. Through the design of the post-processing schedule, the time required for post-processing the green scaffolds is reduced from the initial 80 hrs to 12 hrs. The compressive strength varies from 41 MPa for a part with ~60% porosity to 157 MPa for a part with no designed porosity. Several batches of 13-93 scaffolds are soaked in a simulated body fluid for different time intervals ranging from 1 week to 6 weeks. The amount of hydroxyapatite formed and subsequent mechanical properties are provided and discussed.

1. Introduction

Scaffolds manufactured using biopolymers are bio-inert and do not initiate an active response from the surrounding tissue to bond with the bone by simultaneously supporting tissue regeneration and gene activation. 45S5 glass, discovered by Hench L.L. in 1969 and popularly known as Bioglass®, was the first glass reported to chemically bond with bone; since then, several compositions have been developed based on this original formulation [1]. The actively researched bioactive materials can be broadly divided into glasses, glass-ceramics and crystalline ceramics. Synthetic hydroxyapatite (HA) is a widely researched ceramic with interesting mechanical properties, but its main limitation lies in its slow resorption and conversion rates. The presence of a heat treatment controlled crystalline phase in glass-ceramic systems increases the mechanical properties of the scaffolds; however, it is reported that the presence of a crystalline phase could reduce the rate of mineralization after implantation [2]. Alternatively, amorphous glasses offer excellent bioactive characteristics and an advanced ability to form an HA layer when exposed to body fluids over anywhere from a few hours to even days, depending on their composition. 13-93 glass, a silicate based bioactive glass, is used in this research work to prepare scaffolds intended for bone repair. A higher amount of SiO_2 content in 13-93 glass, compared to 45S5 glass, could slow down the reaction rates upon implantation. However, promising compressive strengths and elastic modulus values for 13-93 makes it a potential candidate for bone scaffolds, particularly for compressive load bearing applications.

Two well-known ways of fabricating parts using selective laser sintering (SLS) are the direct and indirect methods. Fabricating parts with materials having high melting and sintering temperatures, especially in the case of bioceramics, has proven difficult not only because of the

limitations of the machines but also because of the difficulty of controlling the process parameters during fabrication [3, 4]. An alternative approach is an indirect SLS method, in which a binder either is used to fabricate a negative mold of the required porous structure or is mixed with the ceramic material to use as feedstock to the SLS machine [5-7]. The feasibility of fabricating scaffolds with 13-93 bioactive glass using an indirect SLS method with stearic acid (SA) as the binder was reported in our previous work [8]. In such indirect methods, not only should the binder be completely removed from the sintered part because of the biological application, but also the induced micro porosity should be eliminated as much as possible to improve the mechanical properties of the porous constructs. Therefore, post-processing the fabricated "green parts" becomes crucial in such methods. In fact, post-processing steps also exist for a variety of additive manufacturing techniques such as stereolithography (SLA), 3D printing (3DP), fused deposition modeling (FDM), freeze extrusion fabrication (FEF), and others because of the inability of direct methods to process ceramics for similar reasons. Some of the important parameters that need to be considered for the fabrication of functional parts using such methods include the type of binder used, the actual material components and the thermolysis process [9]. The theory of de-binding has been researched for over two decades with reports on some qualitative and quantitative methods [10-13]. However, several aspects, including the wide range of particle sizes used and the complexity of the parts made using the SLS process, make it difficult to fit such parameters in the proposed quantitative research. Therefore, we used an experimental approach to optimize the time required for heat treatment of "green" porous constructs in order to improve the densification when they are fabricated with different particle size ranges and binder content.

In the current work, we investigate the effect of particle size, binder content, SLS parameters, de-binding and sintering heating rates, and immersion of scaffolds in simulated body fluid (SBF) on the microstructure of the scaffolds and on the compressive resistance of the sintered scaffolds. The materials used and methods of analysis are noted in Section 2. The results obtained, including the variation of compressive strengths with respect to the above-mentioned parameters, are presented in Section 3.

2. Materials and Methods

2.1. Preparation of powder

13-93 bioactive glass (prepared by Mo-Sci Corp., Rolla, MO) with a nominal chemical composition of 53% SiO_2, 4% P_2O_5, 20% CaO, 5% MgO, 6% Na_2O and 12% K_2O (in weight %) was used in this research. The details of the 13-93 glass preparation are available elsewhere in the literature [4]. Two sets of 13-93 glass particles were prepared before mixing with the binder; the first set had an average particle size of ~44 µm, and the average particle size of the second set was ~0.7 µm. The first set of 13-93 glass particles were mixed with SA ($C_{18}H_{36}O_2$, grade HS, Acros Organics, Morris Plains, NJ) and dry ball-milled for 8 hrs with ZrO_2 grinding media to obtain the feedstock powder for the SLS machine containing 22% binder content by weight (hereafter represented as B22). Then, a calculated amount of 13-93 glass from the first set was added to the B22 powder and dry ball-milled overnight to obtain the B18 powder. A similar procedure was used to prepare the B15 powder from B18 powder. The B12 powder was prepared by adding 13-93 glass, from the second set (with an average particle size ~0.7 µm), to the B15 powder and then dry ball-milling overnight. All the calculations were based on the bulk densities

of the powders. Particle size distributions were obtained using a laser diffraction-based particle size analyzer (S3500, Microtrac Inc., Largo, FL). All the powders were examined by differential thermal analysis (DTA) (NETZSCH STA 409, Burlington, MA).

2.2. Selective laser sintering

The fabrication experiments were carried out on a commercial DTM Sinterstation 2000 machine. As mentioned earlier, an indirect SLS method was employed in this study, and a feasible set of SLS parameters conducive to fabricating scaffolds using 13-93/SA powders has already been established in our previous work [8]. All the parts in the current work were fabricated using a layer thickness of 76.2 µm. The part bed and part heater temperatures were maintained at 60°C, which is slightly below the melting point of SA (~69°C). This helps the SA to melt at low laser powers and avoids unnecessary temperature gradients in the part bed. The feed bin temperature was maintained at 35°C. An initial set of experiments was planned each time a powder with reduced binder content was used as feedstock to the SLS machine. Several parts measuring 1 cm x 1 cm x 1 mm were initially fabricated to aid in determining the behavior of the powders, and the appropriate SLS control parameters, while being scanned by the laser beam. Our previous work established that an energy density of 1 cal/cm^2 is required to consolidate successive layers. In this work, as powders with reduced binder amounts were used, the energy density was varied from 3.5 to 1 cal/cm^2 at laser powers of 2W, 3W, 4W and 5W by maintaining the scan spacing at 228.6 µm. The 1 mm thick parts were visually inspected for any delamination, and the workable SLS parameter settings were determined based on the best feature definitions of the1 mm thick parts. The effects of SLS parameters will be discussed in greater detail in Section 3.4.

2.3. Post-processing and analysis

The fabricated green parts were post-processed in a three-stage programmable air furnace (Vulcan Benchtop Furnace, York, PA). Scanning electron microscopy (SEM) (S-570, Hitachi Co., Tokyo, Japan) images of the sintered parts were obtained to analyze the microstructures. A cross-head speed of 0.5 mm/min was used on a mechanical load frame (Instron 4469 UTM, Norwood, MA) to determine the compressive strengths of the parts. Five samples in each set were used, and the results are reported as the average value ± the standard deviation. Scans were run from 2θ values ranging from 10° to 80° using Cu Kα radiation (λ = 0.154056 nm) for powder X-ray diffraction (XRD) analysis (Philips X-Pert, Westborough, MA) on the sintered scaffolds and also on the dried scaffolds after removing them from the SBF to determine the crystalline/amorphous nature of the material.

3. Results and Discussion

3.1. Powder characterization for the SLS process

As explained in Section 2.1, the particle size distribution was achieved by dry ball-milling the powders using ZrO_2 grinding media. The graphical representation of the particle sizes is shown in Figure 1. The D50 particle size used in our previous work with B22 powders was ~42 µm. The B22 powder was dry ball-milled so that the D50 particle size decreased to ~24 µm

in the current study; consequently, the layer thickness used in this study was reduced to 76 µm, from the 102 µm thickness used in our previous study. Figure 1 shows the distribution for the B18 powders, which is similar to a bimodal distribution with broad peaks at 10 µm and 44 µm. Improved compaction in the part bed would be obtained with this kind of distribution while spreading the powder in the SLS machine. It was expected in the preparation of the B15 powder that adding 13-93 glass particles to the B18 powder and dry ball-milling overnight would reduce the particle size. The peak in this case was shifted to 10 µm, however, with a significant amount of particles greater than 20 µm, which can be observed in its distribution shown in Figure 1. 13-93 glass particles with an average particle size of ~0.7 µm were added to the B15 powder and then dry ball-milled overnight to obtain the B12 powder. The B12 particle size distribution showed 30% of the particles to be less than 5 µm and 70% of the particles to be less than 20 µm. The mean particle size values of the B18, B15 and B12 powders were 31 µm, 28 µm and 18 µm, respectively. Therefore, it can be said that the mean particle size would not be a correct representation of the wide distribution of particle size ranges for the powders. This makes it difficult to include the particle size parameter in the quantitative approaches for the theory of de-binding because the powders behave differently during the heating cycles, as will be discussed later in the paper. The powders used to fabricate green parts are summarized in Table 1.
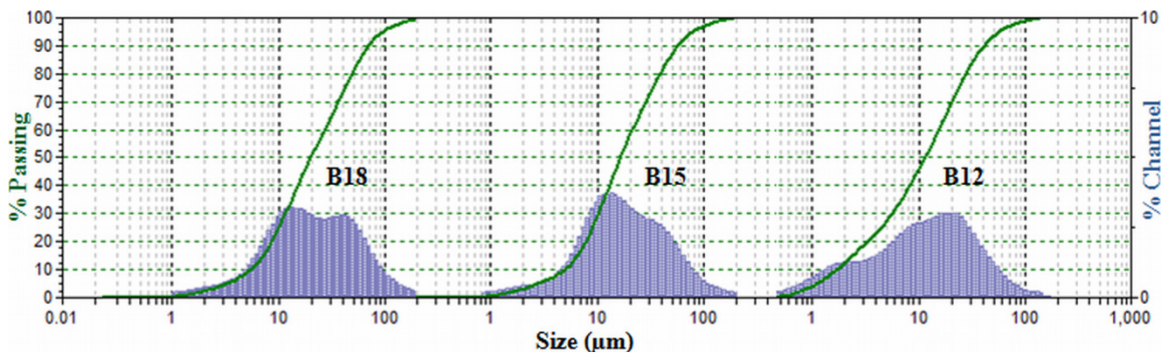

Figure 1. Particle size distributions for powders with different binder contents.

Table 1. Powder characterization

Powders	D50 (µm)	D95 (µm)	Mean (µm)
B18	20	96	31
B15	16	79	28
B12	11	56	18

3.2. Effect of heating rates

The parts fabricated with the SLS parameters mentioned above, and using the B22 powder, are shown in Figure 2. Figure 2(a) shows the green parts, while the sintered parts are shown in Figure 2(b). The parts fabricated include a designed porous part (60% porosity), a hollow part (wall thickness of 1.1 mm and 4
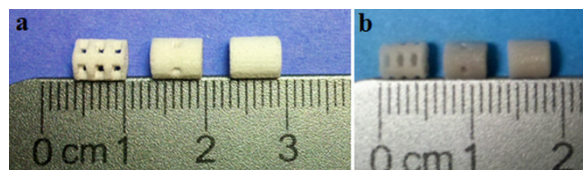

Figure 2. (a) green parts (b) sintered parts

symmetric holes measuring 1.2 mm in diameter) and a solid part with no designed porosity. All parts measured 6 mm in length and 5 mm in diameter. Hereafter, these parts will be referred to as porous, hollow and solid parts. Several batches of the hollow parts were fabricated to study the effect of heating rates on the microstructures, as well as on the compressive strength of the parts. The DTA/TGA analysis of the powders showed complete decomposition of the SA binder at ~540°C. Therefore, the heat treatment of the green parts was completed in two phases: (i) a slower heating rate for de-binding the green parts from room temperature to 550°C and (ii) a relatively faster heating rate until reaching 700°C, with a1 hr hold for sintering of the glass particles followed by a furnace cool to room temperature. Two different sets of experiments were carried out to identify the best possible heating rates for both phases. In the first set of experiments, the sintering rate was kept constant at 2°C/min, and the de-binding rates varied from 0.1 to 2°C/min. In the second set of experiments, the effective de-binding heating rate of 1°C/min was chosen, and the sintering rate varied from 2 to 16°C/min. Figure 3 graphically represents the variation of the compressive strengths of the sintered hollow parts at different heating rates. The graphs indicate that the best possible heating rate before and after de-binding would be around 1°C/min and 5°C/min, respectively.
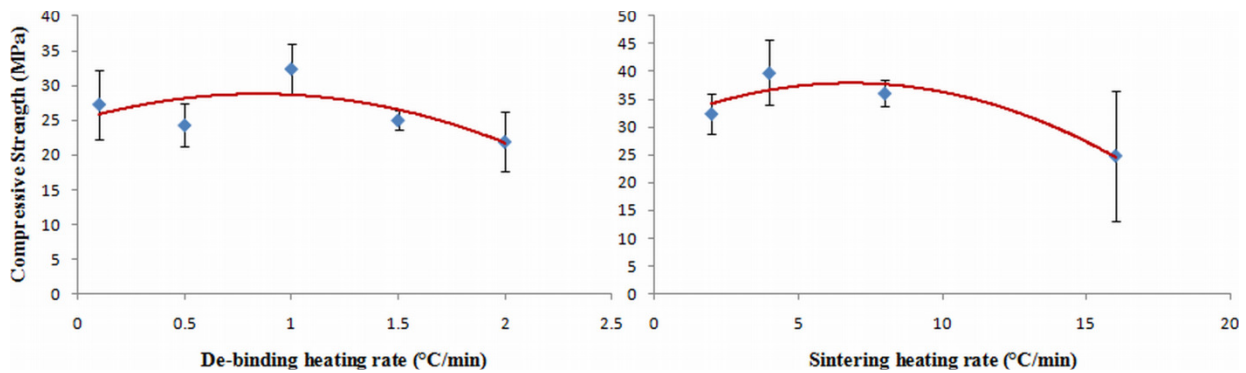

Figure 3. Variation of compressive strength for different de-binding and sintering heating rates for the parts made with B22 powder.

In all the indirect SLS techniques, controlling the heat treatment schedule during post-processing is an essential step. A slow heating rate increases the post-processing time, which could eventually decrease the attractiveness of the method. But, a fast heating rate during de-binding induces micro porosity because of the trapped gases, eventually producing flaws in the microstructure. From the theory of de-binding, it is generally understood that the strength of the parts decreases as the heating rate increases. But, it can be observed from Figure 3 that the strength of the hollow parts increased up to a certain heating rate and then decreased. The faster de-binding heating rate is possible for the porous parts because of larger surface area available for the quicker oxidative decomposition of the SA binder. A further increase in the heating rate would rapidly melt the SA binder causing the porous part to collapse. Even if the part survives, there is the potential for bubble formation in the microstructures. Figure 4 shows the difference in microstructures for de-binding heating rates of 0.1, 1 and 1.5°C/min. In our previous study a 3-day de-binding schedule was developed with holds and variable de-binding heating rates not higher than 0.2°C/min, and the microstructure obtained did not differ significantly from the microstructure obtained with a heating rate of 1°C/min (Figure 4b). Though the difference in compressive strength values is insignificant, this led to a greater reduction in the time required

for post processing. The effect of an increase in sintering heating rates on the compressive strength of the parts has a fairly narrow window of change, though it was observed that 4°C/min gave better results for the hollow parts, possibly because of their finer grain size [14]. A higher heating rate of 16°C/min caused deformation and slumping in the parts, which explains the large standard deviation. However, it must be noted that the heating rates are also dependent on the size of the parts. The developed heating rates were tested on a porous part measuring 1 cm in length and 1 cm in diameter. The applicability of the developed schedule on bigger parts must be investigated further and will be investigated in future studies.
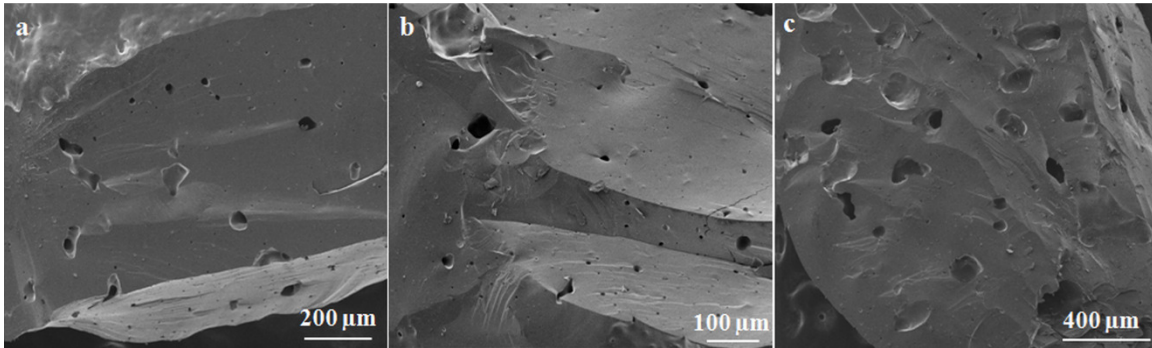

Figure 4. Effect of de-binding heating rates on microstructures (a-c) 0.1, 1 and 1.5°C/min.

3.3. Effect of particle size and binder content

It is known that a smaller particle size range results in a finer, sintered grain size and improved mechanical properties. However, smaller particles have larger surface areas and thus require higher amounts of binder content in the feedstock powder for the SLS machines, which could cause higher shrinkages after heat treatment. Also, smaller particles with higher binder contents are known to cause spreading issues, resulting in warpage during the initial layers of fabrication and may require longer heat treatment schedules. The difficulty in using particle sizes less than 45 µm was reported by Goodridge et al. [16], which could be because of the larger layer thickness used (~ 250 µm), as increased thickness requires a high binder content and higher laser power to melt and join the successive layers. Therefore, a balance must be made between the particle size and the amount of the binder used during SLS fabrication. In our current work, the approach adopted was to decrease the binder content and the particle size simultaneously. In this way, workable parameters of particle size and binder content can be achieved with fewer experiments and less powder waste. Green parts were successfully fabricated using B18 and B15 powders, whereas, the parts made with B12 were fragile to handle and difficulties were experienced while removing the unsintered powder from the pores. Although increasing the laser power to 5W improved the handling of the parts made with B12 powder, it still would not be feasible to handle bigger porous parts in different shapes. Moreover, these parts could not be sintered with the fast heat treatment schedule developed. Therefore, further reduction of binder content from the B12 powders was not considered as it would not be feasible.

To study the variation of mechanical properties for reduced binder content and particle size, several porous, hollow and solid parts were fabricated with the powders prepared, as mentioned in Section 3.1. The heat treatment schedule offering the best results, as discussed in Section 3.2, was used for binder burnout and for sintering the parts. Figure 5 shows

representative porous samples sintered at 700°C for 1 hr (heating at 1°C/min until 550°C and at 5°C/min until 700°C). The results show that the heat treatment schedule was successfully implemented for parts made with the B22, B18 and B15 powders but not with parts made with the B12 powder. According to the theory of thermal de-binding, for the case of oxidative degradation, the de-binding time is inversely proportional to the particle size and packing densities [10]. As mentioned earlier, though the overall particle size range of all the powders is not significantly different, there was in increase

Figure 5. Sintered porous parts made with B22, B18, B15 and B12 powders (L-R).

in the number of particles that were less than 5 µm for the B12 powder, which gives it a better green packing density when compared to the other powders. Therefore, though there is relatively little binder present in the B12 powder, because of the presence of smaller particle sizes, more time would be required for binder burnout; therefore, the accelerated heat treatment schedule did not work for this case. In contrast, higher green densities and wider particle distributions are often useful for better densification during the sintering process. A more appropriate heat treatment schedule for parts fabricated using the B12 powder must be developed with variable heating rates and hold times, which might be expected to take several days. Therefore, considering the poor handleability of these parts, combined with the unsuccessful heat treatment, they did not provide an optimal solution. Table 2 shows the variation of compressive strengths of the porous, hollow and solid parts made with the B22, B18 and B15 powders. Compressive strengths ranged from 18 to 22 MPa for the porous samples, to 41 to 46 MPa for the hollow samples, to up to 115 MPa for the solid samples. As expected, an increasing porosity resulted in a lower strength. Finally, the lowest binder content (B15) resulted in the highest compressive strengths for all three part geometries.
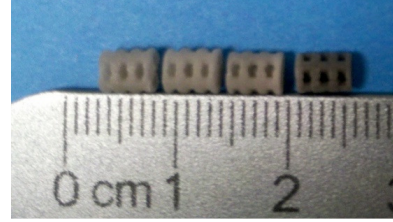
Table 2. Effect of particle size and binder content on compressive strength

Binder content (Wt. %)	Porous (MPa)	Hollow (MPa)	Solid (MPa)
22	18.3±5.8	40.9±6	60.1±24.7
18	19.4±5.4	43.7±12.2	76.9±22.5
15	22.1±3.8	45.9±6.3	115±28.4

3.4. Effect of SLS parameters

Based on their higher overall compressive strengths, the B15 powder was used to study the effect of SLS parameters, again using the developed heat treatment schedule. In the powder-based, indirect AM techniques such as SLS and 3DP, the actual process is only used to fabricate a green part; it is understood that the strength of the sintered part depends on the heat treatment schedule. However, the presence of significant micro porosity in the green part could prove to be detrimental in achieving proper densification during the sintering process. Therefore, it is important to have a compact green part with little or no micro porosity unless the final goal is to achieve built-in porosity in the final sintered parts. In our case, the porosity is designed in the CAD model, so the aim is to achieve maximum densification of the struts in the porous part to improve the mechanical properties of the final sintered part. The powders selected in this work, as explained in Section 3.1, were chosen to reduce the micro porosity in the green parts as much as possible.

The other important component of fabricating the green parts using the SLS process is the melting of the SA binder using a laser beam, which not only has to fuse the successive layers but also has to fill in the voids between the particles to avoid micro porosity in the green parts. This can be achieved through changes in SLS process parameters such as laser power (P), beam speed (BS) and scan spacing (SS). These three important parameters are connected using the following formula: Energy density, ED = P/(BS * SS) [15]. As the laser spot diameter for the DTM Sinterstation 2000 is a constant ~450 µm, scan spacing was kept constant at 228.6 µm, and the other parameters were varied. Therefore, there are two methods to achieve improved melting of the SA binder: (i) increasing the ED at constant P and (ii) increasing P at constant ED. With the first method the sharpness of the features was lost by scanning the beam at low speeds while keeping P constant. This was believed to be due to melting of binder particles adjacent to the part's outline profile through heat transfer. This in turn affected the fabrication of designed porous parts as the adjacent binder particles not scanned by the laser would melt, thereby decreasing the effective pore size in the green part. Therefore, the parameters P and BS were varied accordingly by keeping ED constant at 1 cal/cm^2. A minimum of 3W laser power was required to avoid delamination of the fabricated parts. Increasing the laser power above 3W also melted the SA binder while maintaining the sharpness of the designed features. Figure 6(a) shows the fractured surface of the green part fabricated at 3W laser power using the B22 powder with the D50 particle size ~42 µm. Voids measuring up to ~200 µm in size are indicated in the SEM image. In contrast, a fine distribution of the binder and particle size with no presence of such voids can be observed in Figure 6(b), which is the fracture surface of a part fabricated at 5W laser power using the B15 powder. This is because an increase in laser power could cause the binder in the previously scanned layers to re-melt and distribute itself into any voids present, thereby reducing the micro porosity in the green part. Figure 6(c) shows the fracture surface of a sintered porous part fabricated at 5W laser power using the B15 powder. Similar observations were also made recently by Liu et al. [7], albeit using different materials and for dental applications. Therefore, a uniform distribution of the binder in the green parts leads to a better oxidative degradation during the de-binding stage, thereby improving densification.
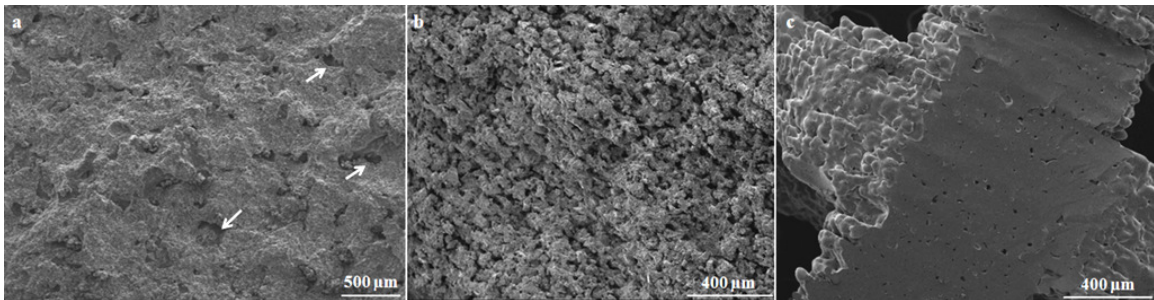

Figure 6. SEM images of the fractured surfaces (a) green part made with B22 powder (b) green part made with B15 powder (c) B15 sintered part showing improved densification.

Figure 7 shows the improvements in the mechanical properties of the porous, hollow and solid parts fabricated at a constant energy density of 1 cal/cm^2 with varying laser powers of 3W, 4W and 5W and corresponding beam speeds of 305, 406 and 508 mm/s. All the parts were made using the B15 powder and were sintered using the schedule developed in Section 3.2. The compressive strength of the porous parts almost doubled, increasing from 22 MPa to 41 MPa, when the laser power was increased from 3W to 5W. Similar trends can also be seen for the hollow and solid parts with the compressive strengths increasing to 61.4 MPa and 157 MPa,

respectively. The compression modulus values for the porous, hollow and solid parts were 4.4±0.7 GPa, 6.1±1.6 GPa and 12±1 GPa, respectively. The modulus values of the porous and hollow parts are similar to that of human trabecular bone and values of solid parts are similar to that of cortical bone [16].
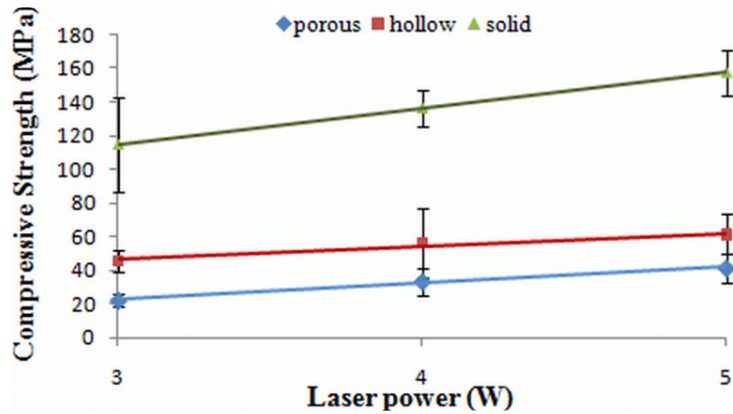

Figure 7. Effect of laser power and beam speed on compressive strength of parts fabricated at a constant energy density of 1 cal/cm^2.

3.5. SBF tests

The SBF solution was prepared based on the Kokubo method [17]. All the samples were ultrasonically cleaned three times using distilled water and then ethanol. The samples were dried in an oven maintained at 65°C overnight and then weighed before being kept in the SBF solution. 100 ml of solution was used for 1 mg of the scaffold. The SBF solution container with scaffolds was kept in an incubator maintained at 37°C. All the compression tests were conducted on wet scaffolds to provide realistic data on the degradation of the scaffolds over different time periods. The variation of the compressive strengths from 1 to 6 weeks is provided in Figure 8. A detailed discussion of the behavior of 13-93 glass and its degradation in SBF can be found
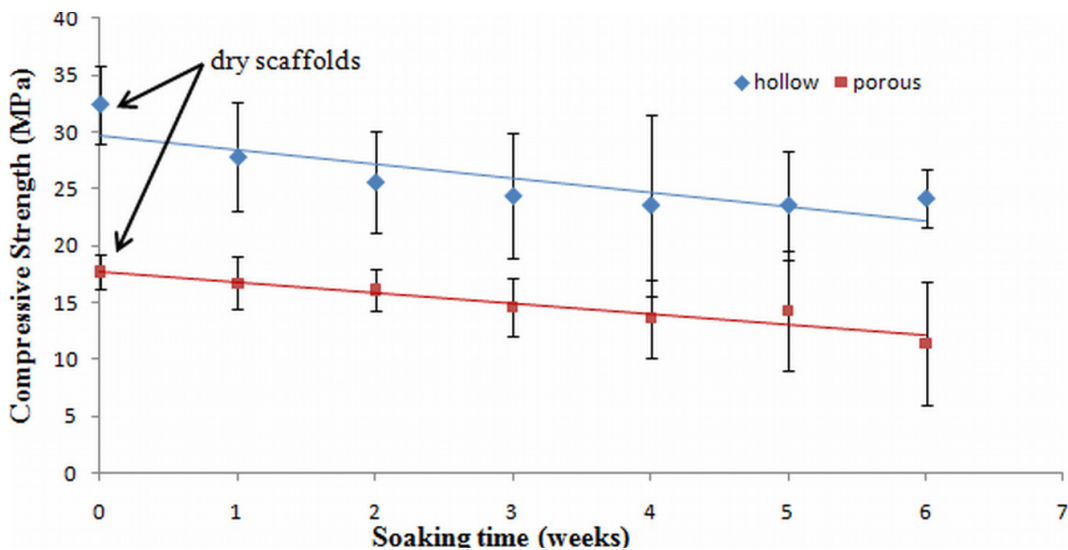

Figure 8. Variation of compressive strength of the samples immersed in SBF.

elsewhere in the literature [18]. The main objective of this work was to study the variation of mechanical properties of the 13-93 glass scaffolds made using SLS method after immersion in SBF. The scaffolds used for this study were made using the B22 powder and the following heat treatment schedule: de-binding heating rate of 1°C/min until 550°C and then heating rate of 2°C/min until the sintering temperature of 700°C was reached. The compressive strength of the porous scaffolds measured after 6 weeks was 11 MPa, approximately 38% reduction, and is at the higher end of the compressive strength of a human trabecular bone [19].

After testing the scaffolds were dried at room temperature, sputter coated with gold-palladium, and investigated using SEM. Specifically, SEM was used to look for HA formation. The HA crystals were formed within a week of the scaffolds' immersion in SBF, which is in accordance with other reports of the in vitro behavior of 13-93 glass [20, 21]. Figure 9 shows the SEM images of two representative scaffolds taken out of the SBF after 2 and 6 weeks, respectively. Figure 9 depicts the typical rough surface morphology of the SLS scaffolds (seen in Figure 6(c)) converting to a smooth surface with a crystalline layer within 2 weeks of immersion. Figure 9(b) shows a fractured surface of a strut of the porous sample after immersion in SBF for 6 weeks. A thick layer, formed by crystals, can be clearly distinguished on the surface of the 13-93 glass in the magnified SEM image shown in Figure 9(c). XRD analysis run on the sample showed a loss of the typical amorphous hump of the 13-93 glass and showed peaks similar to that of HA [4]. The growth and differentiation of osteoblasts on 13-93 scaffolds prepared using other, traditional methods such as polymer foam replication has already been reported [20-22]. Our previous study also showed that 13-93 scaffolds made using SLS process offer vigorous growth of MLO-A5 cells. With improved mechanical properties and SBF test results, combined with the flexibility of manufacturing anatomical shapes as described in the present paper, the indirect SLS process shows its high potential for manufacturing highly interconnected porous structures and load bearing scaffolds for bone repair applications using bioactive glasses.
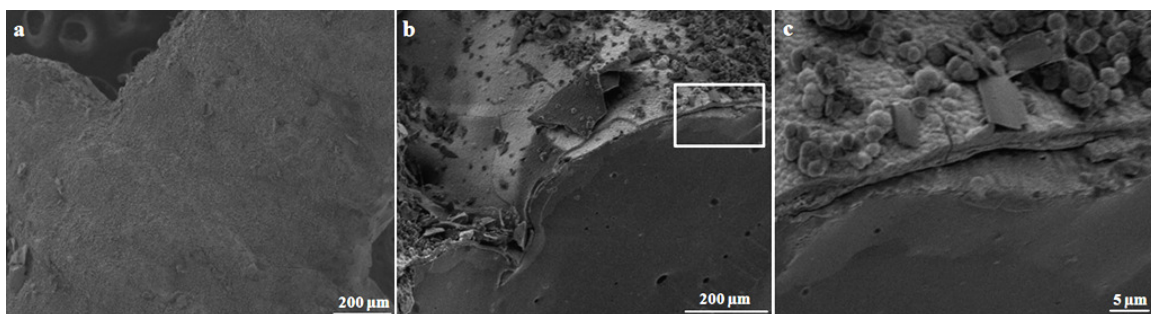

Figure 9. (a) Surface morphology of a porous sample after immersion in SBF for 2 weeks (b) Fracture surface of a porous sample after immersion in SBF for 6 weeks (c) Magnified image showing the growth of HA film on the surface.

4. Summary and Conclusion

The main research objective of this work was to study the effects of material, thermal and SLS process parameters on the mechanical properties of 13-93 bioactive scaffolds manufactured using indirect selective laser sintering (SLS) process. The primary aim of this work was to improve the mechanical properties of 13-93 bioactive scaffolds. This was achieved by reducing the particle size and binder content of the feedstock powder, varying the SLS process parameters

during fabrication and improving the heat treatment schedule of the green parts. The approach used in this work reduced the particle size and the amount of binder content simultaneously. The results showed that the minimum amount of stearic acid binder required to mix with 13-93 glass to obtain a workable feedstock powder for SLS machine was 15% by weight (B15 powder). The particle size distribution with a D50 size of ~16 µm and D95 size of ~79 µm obtained for the B15 powder gave the best possible fabrication results with reduced micro porosity in the green part. The heat treatment schedule developed with a de-binding heating rate of 1°C/min and a sintering heating rate of 5°C/min was based on the highest compressive strengths achieved for the set of experiments as explained in Section 3.2. Although there was an insignificant increase in the mechanical properties, the time required for post processing the green parts was significantly reduced from 80 hrs to 12 hrs. Using the developed heat treatment schedule, the highest compressive strength for the porous sample geometry was achieved for the parts made with B15 powder. Therefore, the B15 powder was used to study the effect of SLS process parameters. It was observed that at a constant energy density of 1 cal/cm^2, increasing the laser power and beam speed from 3W and 305 mm/s to 5W and 508 mm/s had a significant effect on the mechanical properties of the parts. The compressive strength of the porous parts made with B15 powder was further increased to 41 MPa from 22 MPa. However, because of time constraints, SBF tests were carried on the parts made with B22 powder using non-optimized parameters, i.e., fabricated at 3W laser power; 305 mm/s beam speed; 1 cal/cm^2 energy density and post-processed at 1°C/min de-binding heating rate and 2°C/min sintering heating rate. The compressive strengths of these dry porous parts are indicated in the trend of compressive strength vs. soaking time shown in Section 3.5 (see Figure 8). Assuming a similar trend, it can be estimated that the scaffolds with improved mechanical properties (~41 MPa for ~60% porosity) would have a compressive strength ~25 MPa after 6 weeks, which is much higher than the human trabecular bone.

It is concluded that the presence of sub-micron sized particles in the feedstock powder not only increases the post processing time to several days but also requires higher binder content during fabrication. Increasing the laser power and beam speed at a constant energy density during SLS fabrication not only improves the densification in the green part but also preserves the sharpness of the features fabricated when compared to increasing the energy density at a constant laser power and low beam speeds. The compressive strengths of the parts fabricated with the reduced binder content and particle size, improvised heat treatment schedule and SLS parameters varied from 41 MPa for a scaffold with ~60% porosity to 157 MPa for a solid part with no designed porosity. The improved mechanical properties combined with the promising in vitro results show the high potential of scaffolds manufactured with 13-93 bioactive glass using the selective laser sintering process in load bearing applications for bone repair.

References

[1]   Hench L. L. and Wilson J., "*An Introduction to Bioceramics*" (Singapore: World Scientific Publishing Co. Pte. Ltd.) p 47 (1993).

[2]   Rahaman M. N., Brown R. F., Bal B. S. and Day D. E., "Bioactive glasses for nonbearing applications in total joint replacement" *Semin. Arthroplasty* 17 102-12 (2006).

[3]   Lorrison J. C., Goodridge R. D., Dalgarno K. W. and Wood D. J., "Selective laser sintering of bioactive glass-ceramics" *Proc. of the 13th Annual Int. Solid Freeform Fabrication Symp. Austin, TX* 1-8 (2002).

[4]   Kolan K. C. R., Leu M. C., Hilmas G. E. and Velez M., "Selective laser sintering of 13-93 bioactive glass" *Proc. of the 21st Annual Int. Solid Freeform Fabrication Symp. Austin, TX* 504-512 (2010).

[5]   Chu T. M. G., Orton D. G., Hollister S. J., Feinberg S. E. and Halloran J. W., "Mechanical and in vivo performance of hydroxyapatite implants with controlled architectures" *Biomaterials* 23 5 pp. 1283–1293 (2002).

[6]   Goodridge R. D., Dalgarno K. W. and Wood D. J., "Indirect selective laser sintering of an apatite–mullite glass-ceramic for potential use in bone replacement applications" *Proc. Inst. Mech. Eng. H* 220 57-68 (2006).

[7]   Liu J., Zhang B., Yan C. and Shi Y., "The effect of processing parameters on characteristics of selective laser sintering dental glass-ceramic powder" *Rapid Prototyping Journal*, 16 2, pp.138 – 145 (2010).

[8]   Kolan K. C. R., Leu M. C., Hilmas G. E., Brown R. F. and Velez M., "Fabrication of 13-93 bioactive glass scaffolds for bone tissue engineering using indirect selective laser sintering" *Biofabrication* 3 2 (2011).

[9]   Lewis J. A., "Binder removal from ceramics" *Annu. Rev. Mater. Sci.* 27 147–73 (1997).

[10]   German R. M., "Theory of Thermal Debinding" *Int. J. Powder Metall.* 23 4, pp. 237-245 (1987).

[11]   Pinwill I. E., Edirisinghe M. J. and Bevis M. J., "Development of temp-heating rate diagrams for the pyrolytic removal of binder used for powder injection moulding" *Journal of Materials Science* 27 16 4381-4388 (1992).

[12]   Lombardo S. J. and Feng J. C., "Determination of the min time for binder removal and optimum geometry for 3d porous green bodies" *J. Am. Ceram. Soc.*, 86 12 2087–92 (2003).

[13]   Lei Z., Chao Z. K., You L. Z., Yong Z. X., "Degradation and the kinetics of binder removal" *Metal Powder Report* 61 11 28-33 (2006).

[14]   Rahaman M. N., "*Ceramic Processing*" (New York: Taylor and Francis) p 387 (2006).

[15]   Nelson J. C., "Selective laser sintering: A definition of the process and an empirical sintering model" *Dissertation (PhD), University of Texas, Austin* (1993).

[16]   Cowin S. C., "*Bone Mechanics Handbook: Second Edition*" (New York: CRC press) p 10-1 and 15-1 (2000).

[17]   Kukobo T. and Takadama H., "How useful is SBF in predicting in vivo bone bioactivity?" *Biomaterials* 27 15 2907-2915 (2006).

[18]   Fu Q., Rahaman M. N., Fu H. and Liu X., "Silicate, borosilicate, and borate bioactive glass scaffolds with controllable degradation rate for bone tissue engineering applications. I. Preparation and in vitro degradation" *J. Biomed. Mater. Res.* 95A 1 164-171 (2010).

[19]   Carter D. R. and Hayes W. C., "Bone compressive strength: the influence of density and strain rate" *Science* 194 1174–76 (1976).

[20]   Fu Q., Rahaman M. N., Huang W., Day D. E. and Bal B. S., "Preparation and bioactive characteristics of a porous 13-93 glass, and its fabrication into the articulating surface of a proximal tibia" *J. Biomed. Mater. Res.* 82A 222-9 (2007).

[21]   Fu Q., Rahaman M. N., Bal B. S., Brown R. F. and Day D. E., "Mechanical and in vitro performance of 13–93 bioactive glass scaffolds prepared by a polymer foam replication technique" *Acta Biomater.* 4 1854-64 (2008).

[22]   Brown R. F., Day D. E., Day T. E., Jung S., Rahaman M. N. and Fu Q., "Growth and differentiation of osteoblastic cells on 13–93 bioactive glass fibers and scaffolds" *Acta Biomater.* 4 387-396 (2008).